

Conditional, Genetically Encoded, Small Molecule–Regulated Inhibition of NFκB Signaling in RPE Cells

Khiem T. Vu,¹ Fang Zhang,¹ and John D. Hulleman^{1,2}

¹Department of Ophthalmology, University of Texas Southwestern Medical Center, Dallas, Texas, United States

²Department of Pharmacology, University of Texas Southwestern Medical Center, Dallas, Texas, United States

Correspondence: John D. Hulleman, University of Texas Southwestern Medical Center, 5323 Harry Hines Boulevard, Dallas, TX 75390-9057, USA;

John.Hulleman@

UTSouthwestern.edu.

Submitted: April 27, 2017

Accepted: July 18, 2017

Citation: Vu KT, Zhang F, Hulleman JD. Conditional, genetically encoded, small molecule–regulated inhibition of NFκB signaling in RPE cells. *Invest Ophthalmol Vis Sci.* 2017;58:4126–4137. DOI:10.1167/iovs.17-22133

PURPOSE. Nuclear factor κB (NFκB) is a ubiquitously expressed, proinflammatory transcription factor that controls the expression of genes involved in cell survival, angiogenesis, complement activation, and inflammation. Studies have implicated NFκB-dependent cytokines or complement-related factors as being detrimentally involved in retinal diseases, thus making inhibition of NFκB signaling a potential therapeutic target. We sought to develop a conditional and reversible method that could regulate pathogenic NFκB signaling by the addition of a small molecule.

METHODS. We developed a genetically based, trimethoprim (TMP)-regulated approach that conditionally inhibits NFκB signaling by fusing a destabilized dihydrofolate reductase (DHFR) domain to an inhibitor of NFκB, IκBα, in ARPE-19 cells. We then challenged ARPE-19 cells with a number of stimuli that have been demonstrated to trigger NFκB signaling, including LPS, TNFα, IL-1α, and A2E. Western blotting, electrophoretic mobility shift assay, quantitative PCR, ELISA, and NFκB reporter assays were used to evaluate the effectiveness of this DHFR-IκBα approach.

RESULTS. This destabilized domain approach, coupled with doxycycline-inducibility, allowed for accurate control over the abundance of DHFR-IκBα. Stabilization of DHFR-IκBα with TMP prevented IL-1α-, A2E-, LPS-, and TNFα-induced NFκB-mediated upregulation and release of the proinflammatory cytokines IL-1β and IL-6 from ARPE-19 cells (by as much as 93%). This strategy is dosable, completely reversible, and can be cycled “on” or “off” within the same cell population repeatedly to confer protection at desired time points.

CONCLUSIONS. These studies lay the groundwork for the use of destabilized domains in retinal pigment epithelium (RPE) cells *in vivo* and in this context, demonstrate their utility for preventing inflammatory signaling.

Keywords: NFκB, IκBα, destabilized domain, retinal pigment epithelium, inflammation

Nuclear factor κB (NFκB), a proinflammatory transcription factor, is fundamental to cellular innate immunity, and plays a central role in orchestrating an effective inflammatory response in the face of pathogenic and host-derived insults.¹ At the ocular surface, it is clear that NFκB is required to neutralize bacterial and viral pathogens from subsequently compromising the eye and vision.² However, mounting evidence suggests that aberrant, uncontrolled activation of NFκB in the retina may impact many forms of retinal degeneration.³ Yet methods to conditionally and specifically target NFκB signaling within certain cell layers in the retina are lacking. In this study, we sought to identify a genetically based, regulatable approach to limit NFκB signaling and validate its use in retinal pigment epithelium (RPE) cells.

NFκB activation is initiated by exposure to diverse stimuli such as interleukins (e.g., IL-1α, IL-1β), tumor necrosis factors (e.g., TNFα), or bacteria-derived cell wall components (e.g., lipopolysaccharide [LPS]). In turn, activated NFκB increases the synthesis of complement-related genes (e.g., complement component 3⁴) as well as cytokines, such as IL-1β⁵ and IL-6.⁶ Additionally, NFκB activation provides the “priming step” for subsequent inflammasome assembly and release of mature forms of these cytokines.⁷ Classical initiation of NFκB activation originates by engagement of the aforementioned diverse stimuli

with cell surface receptors, such as the IL-1 receptor (IL-1R), TNF receptor 1, or the toll-like receptor (TLR) 2/4.⁸ Activation of these receptors leads to phosphorylation, ubiquitination, and degradation of the inhibitor of NFκB, IκBα. Without IκBα, NFκB translocates to the nucleus wherein it induces transcriptional upregulation of inflammatory cytokines. Interestingly, IκBα is transcriptionally regulated by NFκB,⁹ thus providing a negative feedback loop for subsequently repressing NFκB activity by removing it from the nucleus.¹⁰

Transient activation of NFκB under conditions of microbial or viral invasion is necessary to produce a cytoprotective inflammatory response that, due to feedback mechanisms, eventually resolves upon eradication of the insult.¹¹ However, chronic, unregulated activation of NFκB has been linked to several inflammatory states, such as atherosclerosis,¹² inflammatory bowel disease,¹³ arthritis,¹⁴ and cancer.¹⁵ Similarly, constitutive inflammasome activity is also correlated with a pathologic inflammatory state in diseases such as Alzheimer's disease,¹⁶ gout,¹⁷ and age-related macular degeneration (AMD).¹⁸ Therefore, inhibition of either NFκB “priming” or inflammasome assembly has the potential to ameliorate phenotypes linked to many forms of chronic inflammation or even complement activation.⁷

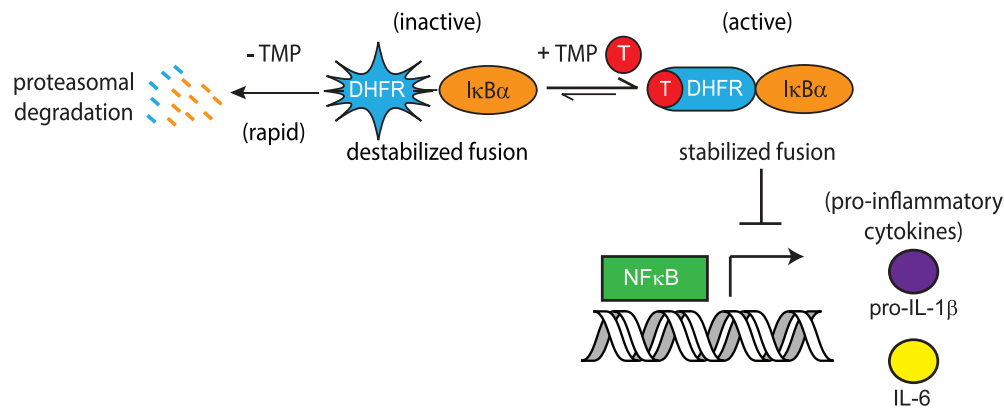


FIGURE 1. Overview of the destabilized domain DHFR approach for reducing NFκB-mediated proinflammatory signaling. In the absence of the small-molecule pharmacologic stabilizer, TMP, cells degrade DHFR along with its fusion protein, IκBα, via ubiquitin-mediated proteasomal degradation. After addition of TMP, DHFR-IκBα is stabilized and is able to conditionally prevent NFκB nuclear translocation and signaling.

Increasing evidence links retinal degeneration and age-related retinal decline with classic markers of inflammasome activation. For example, the RPE from AMD patients with geographic atrophy or neovascularization exhibits increased nucleotide-binding oligomerization domain-like receptor family pyrin domain-containing 3 (NLRP3) staining at diseased sites.¹⁹ Moreover, components of drusen, such as oxidized low-density lipoprotein,²⁰ double-stranded RNA,²¹ and amyloid β,¹⁶ are known activators of either NFκB priming or inflammasome assembly. Furthermore, N-retinylidene-N-retinyl-ethanolamine (A2E), the major phototoxic fluorescent component of lipofuscin, has been found to prime and activate the NLRP3 inflammasome in RPE cells, resulting in significant amounts of IL-1β production in isolated retinal cells and in Stargardt disease mice that lack ATP binding cassette subfamily A member 4 (*Abca4*).²² We have chosen to focus on developing an approach for inhibiting the proinflammatory “priming” activity of NFκB in cultured human RPE cells as a proof of principle, while envisioning that this approach may ultimately serve as a potential therapeutic strategy for treating retinal diseases characterized by chronic inflammation.^{19,23} Although a plethora of pharmacologic NFκB inhibitors exist, the necessity for repeated intraocular delivery of these drugs, their lack of specificity for particular cell layers within the retina, and their potential for off-target effects²⁴ limits their utility. Furthermore, unregulated constitutive repression of NFκB is predicted to be detrimental to RPE viability upon oxidative challenge.^{25,26}

To circumvent these potential issues, we reasoned that we could use a destabilized domain-based approach to control the steady-state protein levels (and therefore the inhibitory activity) of IκBα in a small molecule (trimethoprim [TMP])-dependent manner, as previously accomplished with multiple other transcription factors and signaling proteins.^{27–31} We developed a genetically encoded, small molecule-dependent, reversible strategy for inhibition of NFκB signaling that uses a destabilized domain of *Escherichia coli* dihydrofolate reductase (DHFR) fused to IκBα. In the absence of a small-molecule stabilizer, TMP, the fusion protein is ubiquitinated and degraded by the proteasome.³² However, in the presence of TMP, the DHFR-IκBα fusion protein is stabilized and can prevent NFκB signaling (Fig. 1). This strategy prevented IL-1α, A2E-, LPS-, and TNFα-induced, NFκB-mediated upregulation and release of the proinflammatory cytokines IL-1β and IL-6 from human immortalized RPE cells (ARPE-19) in a small molecule-dependent fashion. This approach is dosable, completely reversible, and can be cycled “on” or “off” repeatedly. We envision that conditional inhibition of NFκB using this method could eventually be used as a novel way to

prevent inflammatory processes associated with retinal degeneration, while minimizing the potential pleiotropic effects associated with direct small-molecule inhibitors of NFκB or constitutive NFκB inhibition.

MATERIALS AND METHODS

Plasmids

A human cDNA clone of wild-type IκBα was purchased from DNASU (Tucson, AZ, USA), amplified, and inserted into pENTR1A DHFR-YFP³⁰ using the SphI and EcoRV restriction sites (replacing YFP with IκBα). DHFR-YFP and DHFR-IκBα were shuttled into a tetracycline/doxycycline-inducible pLenti CMV/TO destination vector by an LR Clonase II reaction (Life Technologies, Carlsbad, CA, USA).

Cell Culture

Vesicular stomatitis virus glycoprotein G (VSV-G)-pseudotyped lentivirus was made by co-transfecting HEK-293T cells with the pLenti CMV/TO constructs along with PAX2 and VSV-G plasmids. Viral supernatants were collected and equal amounts of the supernatants were used to infect ARPE-19 TR (“Tet-On”) cells (described previously³³). Stable, heterogeneous cell populations were generated by selection with puromycin (1 μg/mL; A.G. Scientific, San Diego, CA, USA) for >2 weeks. Cell cultures were routinely screened for mycoplasma (MycAlert Plus, Lonza, Walkersville, MD, USA). Stable NFκB ARPE-19 reporter cells were generated by cotransfecting cells with a plasmid encoding for 5xNFκB responsive elements driving the expression of a secreted luciferase, *Gaussia* luciferase (GLuc, plasmid called “5NF-GLuc” here onward, described previously³⁴) and a constitutively expressed green fluorescent protein (GFP) along with a pLKO puro shSCRAM vector (Sigma-Aldrich Corp., St. Louis, MO, USA) followed by puromycin selection and flow cytometry-assisted cell sorting based on GFP signal. Human IL-1α and human TNFα were purchased from PeproTech (Rocky Hill, NJ, USA), LPS was purchased from Sigma-Aldrich Corp., 4-HNE was purchased from Enzo (Farmingdale, NY, USA), and A2E was purchased from Gene and Cell Technologies (Vallejo, CA, USA).

Western Blotting

For typical Western blotting experiments, (e.g., Fig. 2J–L), cells were plated at 200,000 cells per well of a 12-well plate in complete Dulbecco’s modified Eagle’s medium (DMEM)/F12

media containing 10% serum. The next day, cells were treated as indicated. For Western blotting involving production of cytokines, ARPE-19 cells were plated as described above followed by gradual serum removal over the course of a week until the serum was removed completely followed by indicated treatments. At appropriate time points, ARPE-19 cells were lysed in-plate with either radioimmunoprecipitation assay (RIPA) buffer (50 mM Tris, pH 7.4, 150 mM NaCl₂, 1% Triton X-100 [vol/vol], 0.1% SDS [wt/vol], 0.5% sodium deoxycholate [wt/vol]) supplemented with Halt Protease and Phosphatase inhibitors (Pierce, Rockford, IL, USA) and benzonase (Sigma-Aldrich Corp.) or a buffer containing 50 mM HEPES pH 8, 10 mM KCl, 2 mM MgCl₂, and 1.0% SDS also supplemented with benzonase. Cells were lysed at RT for approximately 1 to 2 minutes, followed by freezing at -80°C . Lysates were thawed on ice and spun at 21,000g for 5 to 10 minutes at 4°C . The supernatant was collected and subjected to a bicinchoninic acid assay (BCA; Pierce). Where indicated, nuclear extracts were obtained by using the NE-PER kit (Pierce). Samples were denatured in Laemmli buffer with reductant, followed by loading on a 4% to 20% Tris-Glyc SDS-PAGE gel. Proteins were transferred to a nitrocellulose membrane using a G2 Fast Blotter (Pierce) or iBlot2 (Life Technologies). Blots were typically dried for ≥ 1 hour at RT before staining with Ponceau S (Sigma-Aldrich Corp.) and blocking (LI-COR, Lincoln, NE, USA). Blots were then probed with one or more of the following antibodies: mouse anti-GFP (1:3000; Santa Cruz, Dallas, TX, USA), rabbit anti-IκBα (1:1000; Santa Cruz), mouse anti-phospho-IκBα (S32, 1:500; Santa Cruz), mouse anti-phospho-IKKα/β (S176/S180, 1:1000; Cell Signaling, Danvers, MA, USA), rabbit anti-IKKα (1:500; Santa Cruz), mouse anti-NFκB (p65, 1:500; Santa Cruz), rabbit anti-phospho-NFκB (p65, S536, 1:500; Santa Cruz), mouse anti-GAPDH (1:3000; Santa Cruz), mouse anti-IL-1β (1:1000; Cell Signaling), mouse anti-IL-6 (1:500; Santa Cruz), mouse anti-IL-18 (1:500; Santa Cruz), or rabbit anti-matrin-3 (Bethyl Laboratories, Montgomery, TX, USA). An appropriate LI-COR anti-mouse or anti-rabbit IR-conjugated secondary was used. All blots were imaged and quantified on a LI-COR Odyssey CLx.

NFκB Electrophoretic Mobility Shift Assay (EMSA)

Cells were plated at a density of 500,000 cells per well of a six-well plate and treated with media containing DMSO or dox/TMP for 48 hours before stimulation with IL-1α (25 ng/mL) for an additional 24 hours (in the presence of DMSO or dox/TMP). Nuclear fractionation and lysis were accomplished as described previously.³⁵ Nuclear lysates (5 μg) were incubated with 0.5 to 1.0 μL IRDye 700 NFκB probe (LI-COR) in binding buffer (10 mM Tris pH 7.5, 50 mM KCl, 3.5 mM DTT, 0.25% Tween 20, poly[dI*dC]) for 30 minutes at RT. Samples were then run on a non-denaturing 4% polyacrylamide gel in 0.5x Tris/Borate/EDTA buffer until resolved. The resulting gel was visualized on a LI-COR Odyssey CLx.

Quantitative PCR (qPCR)

Cells were harvested by trypsinization, washed, and frozen at -80°C for at least 1 hour before use. mRNA was then extracted from cell pellets using an Aurum Total RNA kit (BioRad, Hercules, CA, USA). Although we did not assess the quality of every RNA preparation, with this method of isolation we routinely obtain RNA integrity numbers of >8.9 (TapeStation 2200; Agilent Technologies, Santa Clara, CA, USA). A total of 100 ng RNA was reverse transcribed with qScript cDNA SuperMix (Quanta Bioscience, Beverly, MA, USA). cDNA was diluted ≥ 5 -fold with water, and analyzed using TaqMan probes and TaqMan Advanced Fast Master Mix (Life Technologies).

The probes used were as follows: human β-actin (Hs03023880), human IκBα (Hs00355671), human IL-1β (Hs00174097), human IL-6 (Hs00985639), and human IL-18 (Hs01038788), all from Life Technologies.

For array-based work, diluted cDNA was applied to a fast 96-well Human NFκB pathway TaqMan array plate (Life Technologies) and run under fast conditions using the master mix described above. All C(t) values within each plate were normalized to the 18S ribosomal RNA endogenous control, and then plates were compared to each other (IL-1α + dox/TMP versus IL-1α + DMSO) using QuantStudio Real Time PCR Software (Thermo Fisher Scientific, Waltham, MA, USA). $\Delta\Delta\text{C}(t)$ values were calculated and expressed as relative quantities (also known as fold-change). Wells with no C(t) determination after 40 cycles were considered as “not amplified.”

Enzyme-Linked Immunosorbent Assay (ELISA)

Cells were plated at a density of 200,000 cells per well of a 12-well plate in complete DMEM/F12 media containing 10% serum. Over the course of a week, the serum was gradually removed, and after 1 week, serum was removed completely. Cells were then treated with either DMSO or dox/TMP for 48 hours before stimulation with IL-1α, A2E, or a combination thereof for an additional 24 hours in serum-free media. Conditioned media was collected, spun, and frozen at -80°C until further use in an IL-1β Ultrasensitive ELISA (0.31–20 pg/mL; Life Technologies) or IL-6 ELISA (15–1540 pg/mL; Life Technologies). Significant dilutions (up to 1:1000) of some IL-1α-treated samples were required when assaying for IL-6 to fall within the standard curve.

NFκB-Responsive *Gaussia* Luciferase (GLuc) Assay

To indirectly measure NFκB activity, we used a system developed by Badr et al.³⁴ that relies on 5xNFκB responsive elements to drive expression of a secreted luciferase, GLuc. The luciferase assay was performed as described previously using conditioned culture media.^{36–38}

Statistical Analysis

To determine significance for Western blotting (IκBα degradation), qPCR, ELISA (IL-1β, IL-6) or GLuc assays, an unpaired one- or two-tailed *t*-test was used assuming equal variance. For TaqMan gene array values, a one-sample *t*-test was used comparing the values to a hypothetical mean of 1 (i.e., unchanged). Values were determined to be significant when *P* values were less than 0.05.

Supplemental Methods

Viability Assays. Cells were plated in a 96-well plate at a density of 15,000 cells per well in full media. Over the course of 1 week, the serum was gradually lowered and completely removed after 1 week. Cells were incubated in serum-free media for an additional week (for a total of 2 weeks in culture) followed by treatment with either DMSO or dox/TMP for 72 hours. Cells were then analyzed by three different assays: (1) a resazurin mitochondrial reduction potential assay, (2) a lactate dehydrogenase (LDH) release assay (G-Bioscience, St. Louis, MO, USA), and (3) an ATP assay (Cell Titer Glo 2.0; Promega, Madison, WI, USA).

Transepithelial Electrical Resistance (TEER). Cells were plated at a density of 50,000 cells per well on an uncoated, 0.4-μm polyester transwell insert (12-well plate; Corning, Corning, NY, USA). Cells were allowed to polarize and

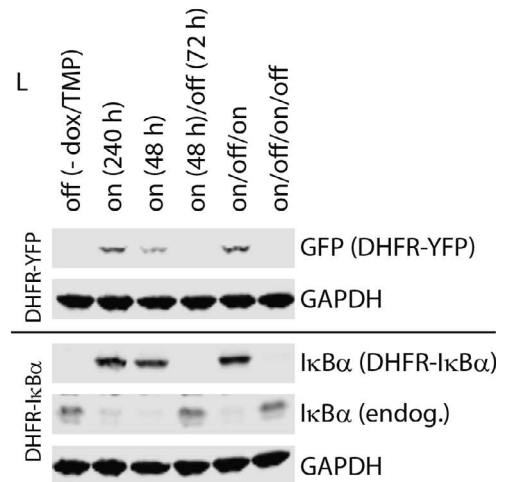
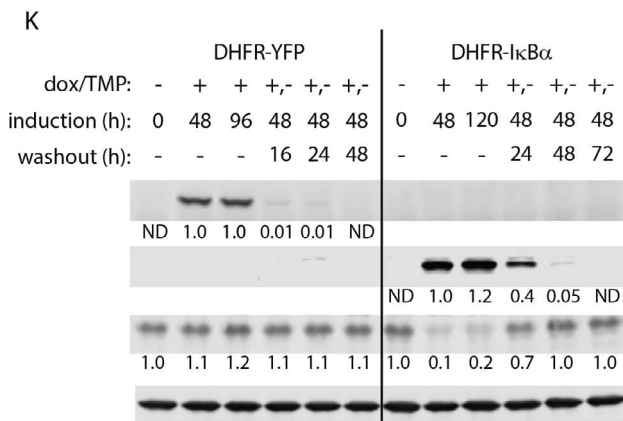
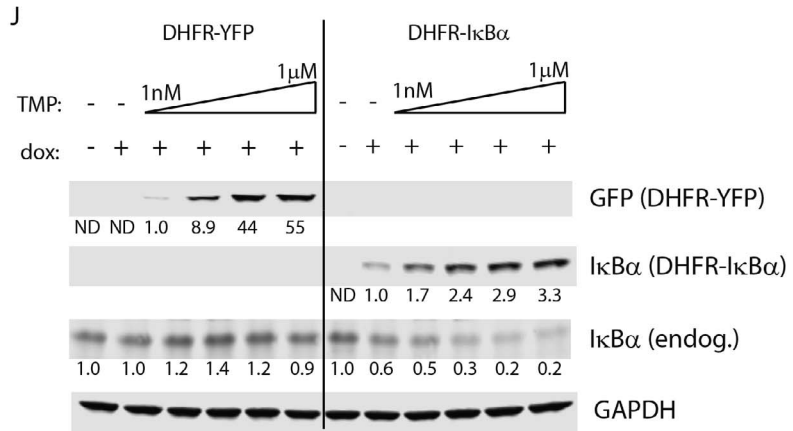
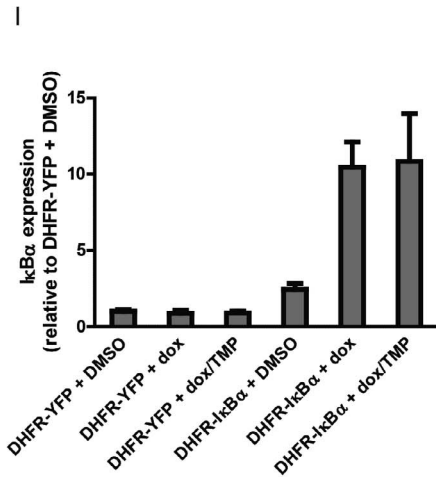
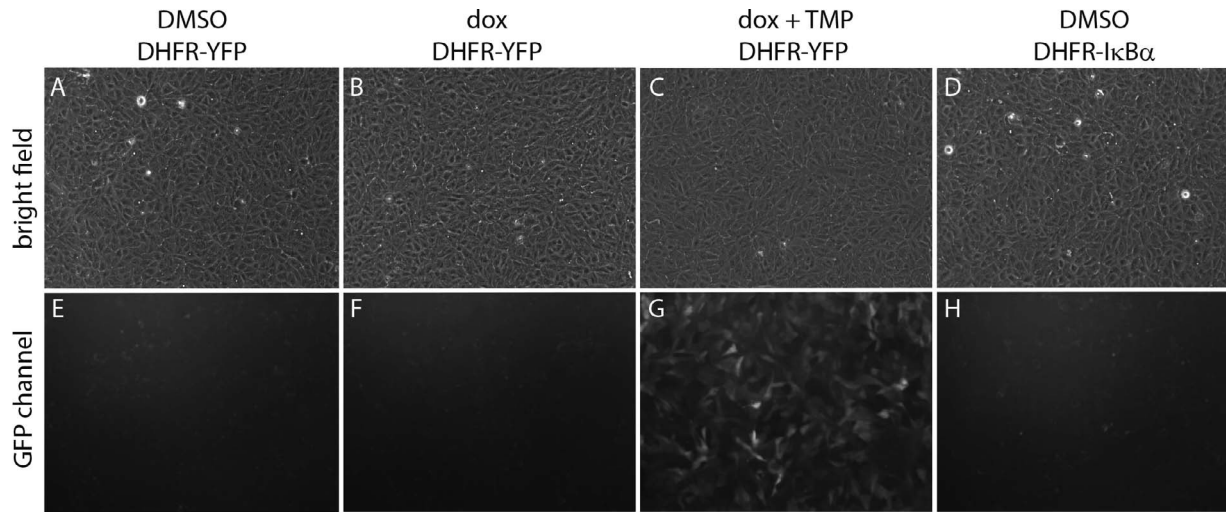


FIGURE 2. Generation of an inducible system to regulate IκBα abundance in ARPE-19 TR cells. Bright-field (A–D) and green fluorescence (E–H) images of DHFR-YFP and DHFR-IκBα stable cells treated with either DMSO, dox (100 ng/mL), or dox combined with TMP (1 μM) for 48 hours. (I) Dox/TMP has no effect on endogenous IκBα expression, and DHFR-IκBα transcript levels are inducible and do not change with TMP addition, mean ± SD. (J) Protein levels of DHFR-YFP and DHFR-IκBα are tightly regulated, inducible, and dose-dependent. ND, not detected. (K) The DHFR-based strategy can be completely turned off after simple removal of dox/TMP within 48 hours (DHFR-YFP) or 72 hours (DHFR-IκBα). (+, –), addition of dox/TMP, then removal. (L) DHFR-YFP and DHFR-IκBα can be repeatedly cycled on and off. Representative data shown of n ≥ 3 independent experiments for all panels.

form tight junctions over the course of a week. TEERs (after blank subtraction) were measured using an EVOM2 meter (World Precision Instruments, Sarasota, FL, USA) and then DMSO or dox/TMP was added to both sides of the transwell. TEERs were re-assessed after 48 hours and the difference between the two readings was calculated.

RESULTS

Validation of the DHFR-Based Destabilized Domain Approach in ARPE-19 Cells

We generated constructs encoding for DHFR-YFP (as a control) and DHFR-IκBα. To confer an additional level of control over our genes of interest, we generated them as doxycycline (dox)-inducible (also known as “Tet-On”) constructs. After lentiviral infection of ARPE-19 TR cells³³ and subsequent stable selection, heterogeneous populations of cells expressing DHFR-YFP (control cells) demonstrated tight regulation of DHFR-YFP expression and stability (Figs. 2A–C, 2E–G, 2J). In the presence of dox alone, neither fluorescence (Fig. 2F) nor fusion protein (Fig. 2J) was detected. However, on addition of dox and TMP, which stabilizes newly synthesized DHFR fusion proteins, YFP fluorescence is detectable (Fig. 2G), as is the protein (Fig. 2J). DHFR-IκBα cells were used as an absolute negative fluorescence control (Figs. 2D, 2H). Under untreated, basal levels, there was a small, approximately 2-fold increase in *IκBα* transcript in DHFR-IκBα cells, indicating slight leakiness of the dox-regulated system (Fig. 2I). However, in the absence of dox, no DHFR-IκBα protein was detectable, and endogenous levels of IκBα were identical to control cells (Fig. 2J). After addition of dox, a large, approximately 10-fold increase in *IκBα* transcript levels was observed (Fig. 2I), and a small amount of DHFR-IκBα was detectable under +dox steady-state levels (Fig. 2J). Although addition of TMP had no effect on DHFR-IκBα transcript levels (Fig. 2I), since TMP stabilization occurs at the protein level, it dose-dependently increased DHFR-IκBα protein levels with the addition of increasing TMP (Fig. 2J). Concomitantly, as DHFR-IκBα was stabilized, endogenous IκBα was reduced in an apparent compensatory autoregulatory mechanism.³⁹ TMP addition (1 nM) to cells expressing DHFR-YFP stabilized the fusion protein such that it was detectable by Western blotting and dose-dependently stabilized DHFR-YFP to a plateau of 1 μM (Fig. 2J).

Next we assessed whether the stabilization of the DHFR fusion proteins was reversible. DHFR-YFP and DHFR-IκBα cells were induced with dox/TMP for 48 hours followed by washing with Hanks’ balanced salt solution and replacement with fresh media lacking dox/TMP for 16 to 72 hours. Sixteen to 24 hours after removal of dox/TMP, DHFR-YFP levels decreased by 99% and were completely undetectable by 48 hours after removal of dox/TMP (Fig. 2K). The DHFR-IκBα fusion protein, however, required a longer period of “washout” to become undetectable. Within 24 hours of dox/TMP removal, only 60% of the fusion protein was degraded (Fig. 2K). This value increased to 95% degradation by 48 hours, and complete degradation by 72 hours of washout (Fig. 2K). Again, endogenous IκBα protein levels were inversely proportional to the levels of stabilized DHFR-IκBα (Fig. 2K). Subsequently, we determined whether our system could be cycled between an “on” (i.e., stabilization of the fusion protein) or “off” (degradation of the fusion protein) state repeatedly. Stabilization of the DHFR fusion proteins was accomplished by 48 hours of dox/TMP followed by a 72-hour washout period, restabilization for 48 hours, and a final 72-hour washout period. Using these parameters, we were able to effectively

cycle both DHFR-YFP and DHFR-IκBα in an “on/off/on/off” manner over the course of a 10-day experiment (Fig. 2L). It is important to note that a 72-hour treatment of the ARPE-19 cells with dox/TMP itself had no effect on cell viability as measured by mitochondrial reduction potential (Supplemental Fig. S1A) or lactate dehydrogenase (LDH) release (Supplemental Fig. S1B). Furthermore, the ATP content of the cells remained unchanged after treatment (Supplemental Fig. S1C) and both the DHFR-YFP and DHFR-IκBα cells did not differ in their ability to form tight junctions and maintain a reasonable TEER (Supplemental Fig. S1D). Finally, the TEER was not compromised by prolonged (48-hour) treatment with dox/TMP (Supplemental Fig. S1E).

DHFR-IκBα Is Regulated Similarly to Endogenous IκBα After IL-1α Administration

We tested whether DHFR-IκBα was properly phosphorylated and turned-over after stimulation with the prototypical inflammatory cytokine, IL-1α (shown previously to activate NFκB signaling⁴⁰ through the IL-1R,⁴¹ and has been used previously in ARPE-19 cells²²). At the protein level, DHFR-IκBα behaved much like endogenous IκBα, albeit at higher overall steady-state levels. Thirty minutes after addition of IL-1α, a portion of DHFR-IκBα was robustly phosphorylated and degraded (Fig. 3A). This degradation was maximal at 1 hour post IL-1α treatment, similar to that of endogenous IκBα in IL-1α-treated DHFR-YFP-expressing cells (Figs. 3A, 3B). The extent of DHFR-IκBα phosphorylation and subsequent degradation paralleled phosphorylation (activation) of the IκB kinase complex (IKK) subunits α/β (Fig. 3A), strongly suggesting that DHFR-IκBα, like endogenous IκBα, is phosphorylated by IKK, which in turn promotes its ubiquitination and degradation.⁴² After 1 hour of treatment, DHFR-IκBα and endogenous IκBα levels began to rebound and reach approximately 1.2-fold over untreated IκBα values by 6 to 24 hours (Figs. 3A, 3B).

Stabilization of DHFR-IκBα Prevents NFκB Nuclear Translocation and Downstream Gene Expression

We tested whether stabilization of DHFR-IκBα prevented IL-1α-induced NFκB nuclear translocation. ARPE-19 cells were pretreated with dox/TMP for 48 hours, followed by treatment with IL-1α for 24 hours, and then subjected to nuclear protein extraction. As we predicted, ARPE-19 cells expressing stabilized DHFR-IκBα demonstrated virtually no nuclear NFκB signal even after IL-1α stimulation (Fig. 4A), demonstrating that it can sequester NFκB in the cytosol in an inactive conformation. Next, we wished to confirm whether stabilized DHFR-IκBα could in fact dampen or prevent NFκB transcriptional signaling. Cells were treated as described above, then harvested and processed for an EMSA using a fluorescently labeled NFκB consensus oligonucleotide. Only in cells treated with IL-1α did we observe a detectable shift in the migration of the NFκB oligonucleotide, an indication of NFκB nuclear translocation and DNA binding (Fig. 4B). Importantly, there was a substantial reduction in the intensity of this band only in cells with stabilized DHFR-IκBα, demonstrating that our strategy can indeed repress IL-1α-induced NFκB nuclear translocation and activity (Figs. 4A, 4B). Furthermore, transcriptional analysis of identically treated cells revealed that stabilization of DHFR-IκBα significantly reduced IL-1α-induced, NFκB-dependent *IL-1β*⁴³ and *IL-6*⁶ transcripts by 90% and 82%, respectively (Figs. 4C, 4D; *P* < 0.01), while having no appreciable effect on *IL-18* levels (Fig. 4E), a gene that is constitutively produced and regulated independently of NFκB.⁴⁴

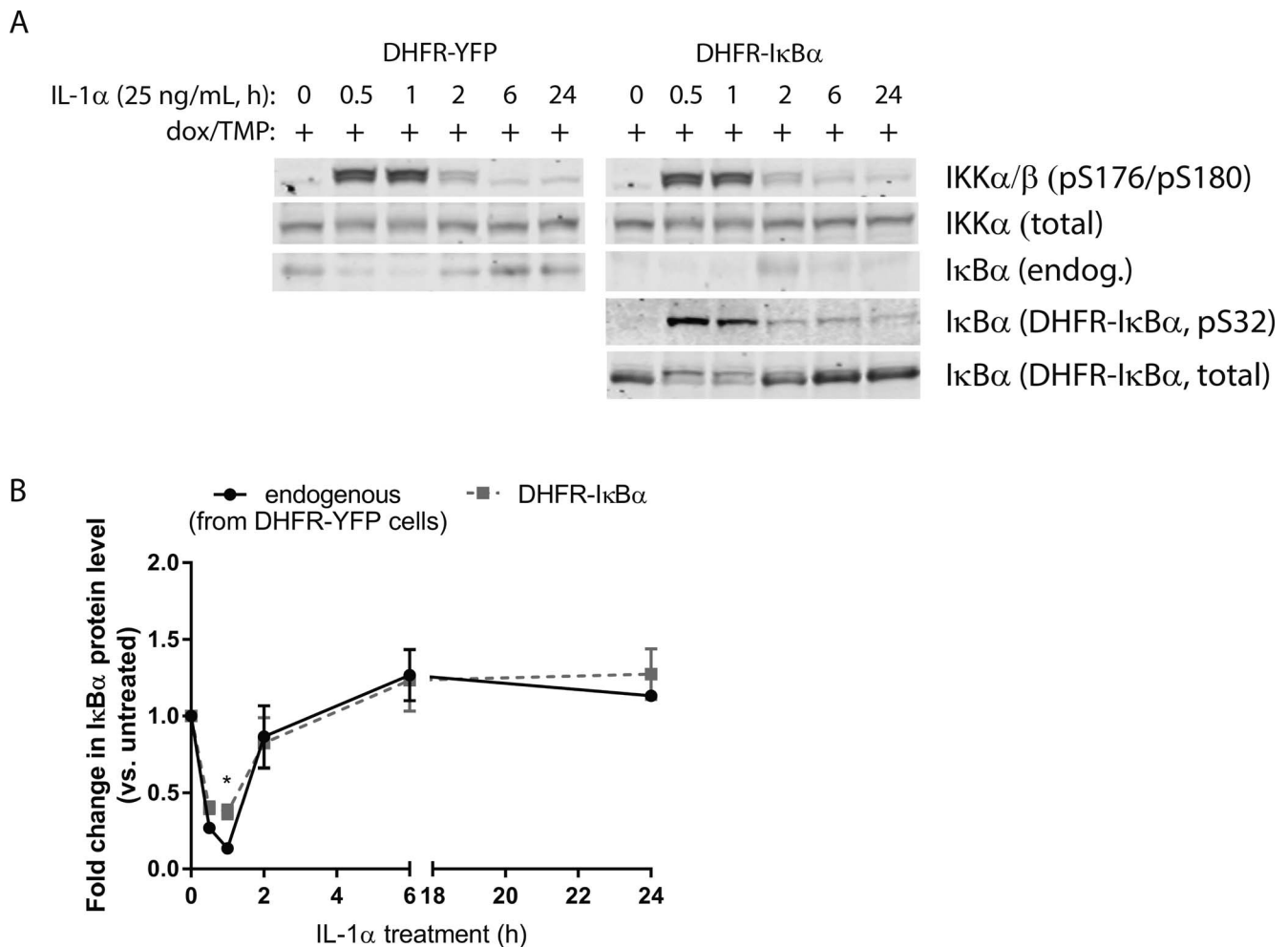


FIGURE 3. DHFR-IκBα can be phosphorylated and degraded similarly to endogenous IκBα. **(A)** DHFR-IκBα is likely phosphorylated by the IKK complex, and a portion can be rapidly degraded, even in the presence of TMP. ARPE-19 cells were treated with IL-1α for the indicated time and whole-cell lysates were harvested. Representative data shown of $n \geq 3$ independent experiments. **(B)** Quantification of the fold-change in IκBα protein levels post cytokine addition. $n = 3$, mean \pm SEM. * $P < 0.05$, unpaired, two-tailed t -test assuming equal variance.

Subsequently, we sought to identify additional NFκB-target genes that were differentially regulated by DHFR-IκBα stabilization by using TaqMan transcriptional arrays. Only one gene of the 93 assayed was identified to be consistently upregulated (≥ 2 -fold in two independent replicates, $P < 0.05$) in IL-1α-stimulated dox/TMP-treated versus IL-1α-stimulated DMSO-treated DHFR-IκBα cells. This gene was the B-cell lymphoma 2 gene (*BCL2*, Fig. 4F). This hit was unexpected; *BCL2* has been demonstrated to be upregulated after NFκB activation.^{45,46} Our data suggest that this gene may be differentially regulated in ARPE-19 cells or under these specific conditions. The vast majority of hits (16) were found to be reduced (≥ 2 -fold decrease, $P > 0.05$) in IL-1α-stimulated dox/TMP versus IL-1α-stimulated DMSO cells (Fig. 4F). These results confirmed our previous observations of *IL-1β* and *IL-6* transcript levels (Figs. 4C, 4D), but also included additional proinflammatory genes, such as *IL-8*, and cell migration mediators, such as vascular cell adhesion molecule 1 (*VCAM1*) and intracellular cell adhesion molecule 1 (*ICAM1*; Fig. 4F). Two genes in particular, *TLR2* and *VCAM1*, were found to be amplified in IL-1α + DMSO-treated cells, but not amplified in either experiment in IL-1α + dox/TMP-treated cells (Fig. 4F), indicating a substantial reduction in the expression of these genes between the two treatments.

Stabilization of DHFR-IκBα Prevents the Production and Release of NFκB-Dependent Cytokines

Our observations of downstream NFκB signaling at the transcriptional level after IL-1α stimulation were also paralleled at the translational level, as indicated by Western blotting (Fig. 5A). In these experiments, we again used IL-1α as a NFκB “priming” stimulus, but also treated cells with N-retinylidene-N-retinylethanolamine (A2E), the main fluorescent component of lipofuscin⁴⁷ and lysosomotropic agent,⁴⁸ which induces the assembly of the NLRP3 inflammasome²² responsible for ultimately cleaving certain pro-cytokines, such as pro-IL-1β and pro-IL-18. IL-1α treatment resulted in phosphorylation of NFκB at Ser536 (pS536), a highly conserved residue that is potently phosphorylated in response to inflammatory stimuli⁴⁹ (Fig. 5A). However, NFκB pS536 is independent of IκBα regulation⁵⁰ and is not necessarily an indication of NFκB activity or translocation.⁵¹ Thus, levels of pS536 NFκB did not differ substantively between DHFR-YFP or DHFR-IκBα under any condition used (Fig. 5A). In contrast, levels of intracellular pro-IL-1β as well as IL-6 after IL-1α or IL-1α/A2E treatment were decreased by a minimum of 90% in ARPE-19 cells with DHFR-IκBα stabilized

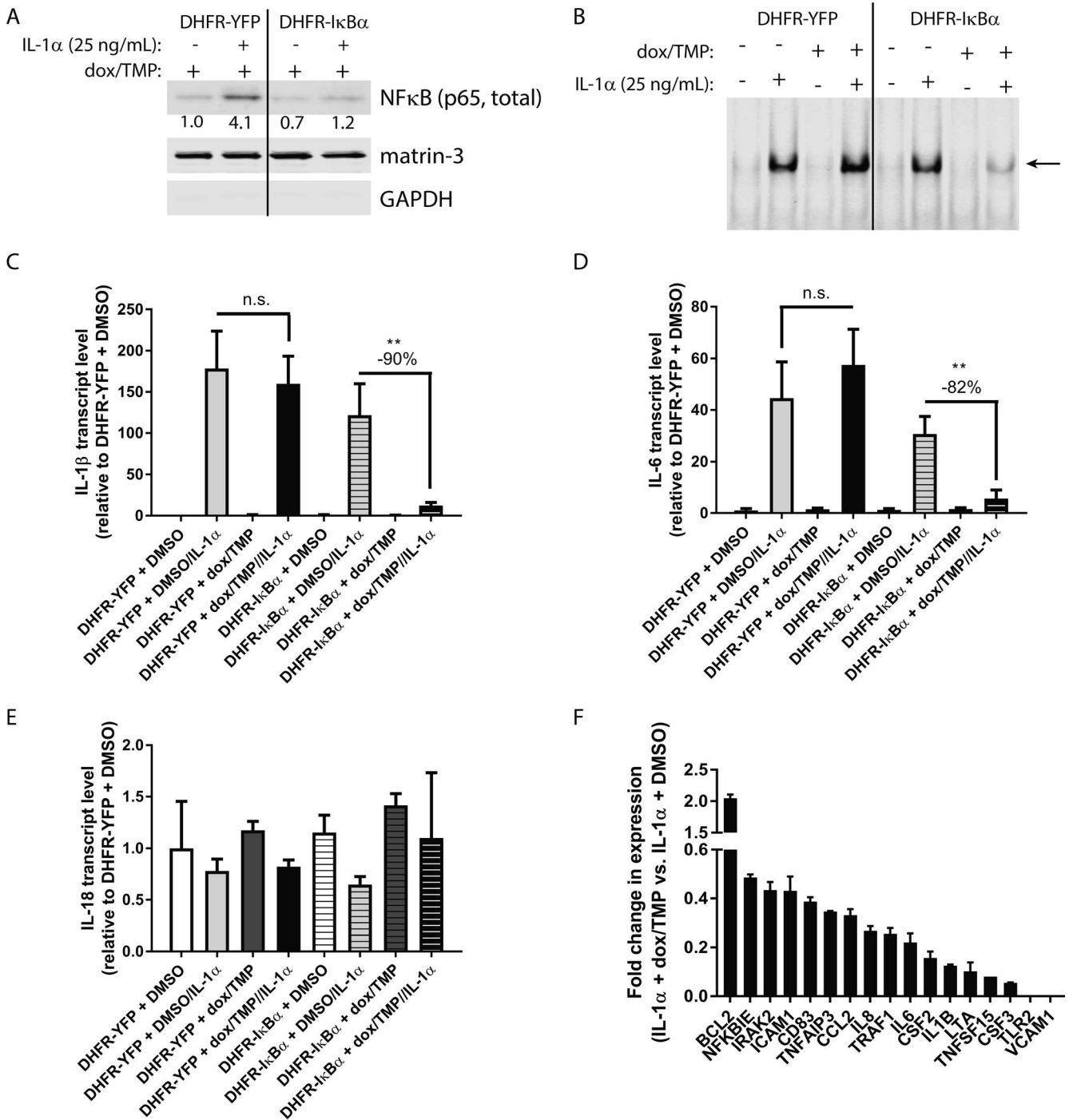


FIGURE 4. Stabilization of DHFR-IκBα inhibits NFκB signaling. ARPE-19 cells were plated and pretreated with DMSO or dox/TMP (100 ng/mL/1 μM) for 48 hours followed by treatment with IL-1α (25 ng/mL) for 24 additional hours for all experiments. (A) Stabilization of DHFR-IκBα prevents NFκB nuclear translocation after IL-1α stimulation. (B) DHFR-IκBα prevents binding of a fluorescently labeled NFκB consensus oligonucleotide to nuclear NFκB as determined by an EMSA. (C, D) Stabilized DHFR-IκBα reduces transcription of classic NFκB-dependent cytokines IL-1β (C) and IL-6 (D). *n* = 3. ***P* < 0.01, unpaired, two-tailed *t*-test assuming equal variance. (E) Transcription of IL-18, an NFκB-independent cytokine, is not increased by IL-1α, nor is it affected by stabilization of DHFR-IκBα. (F) NFκB TaqMan array of genes that are consistently upregulated or downregulated (≥ or ≤ 2-fold, respectively, *P* < 0.05), one-sample *t*-test compared with a hypothetical mean of 1 (i.e., unchanged) in DHFR-IκBα + IL-1α + DMSO versus DHFR-IκBα + IL-1α + dox/TMP. *n* = 2 independent experiments. Note: TNFSF15 was amplified in only one DHFR-IκBα + IL-1α + dox/TMP sample, whereas TLR2 and VCAM1 were not amplified in either DHFR-IκBα + IL-1α + dox/TMP replicate. Representative data shown of *n* ≥ 3 independent experiments for (A-E), mean ± SD for all bar graphs in this figure.

by dox/TMP (Fig. 5A). In fact, levels of IL-6 post stabilization of DHFR-IκBα were not detectable even after IL-1α or IL-1α/A2E treatment (Fig. 5A). A2E alone caused no detectable effects using Western blotting techniques. As expected, levels

of intracellular pro-IL-18 were not changed with any condition tested, regardless of cell line (Fig. 5A).

ELISA was used to monitor changes in secreted canonical NFκB-dependent cytokines. IL-1α increased IL-1β secretion in

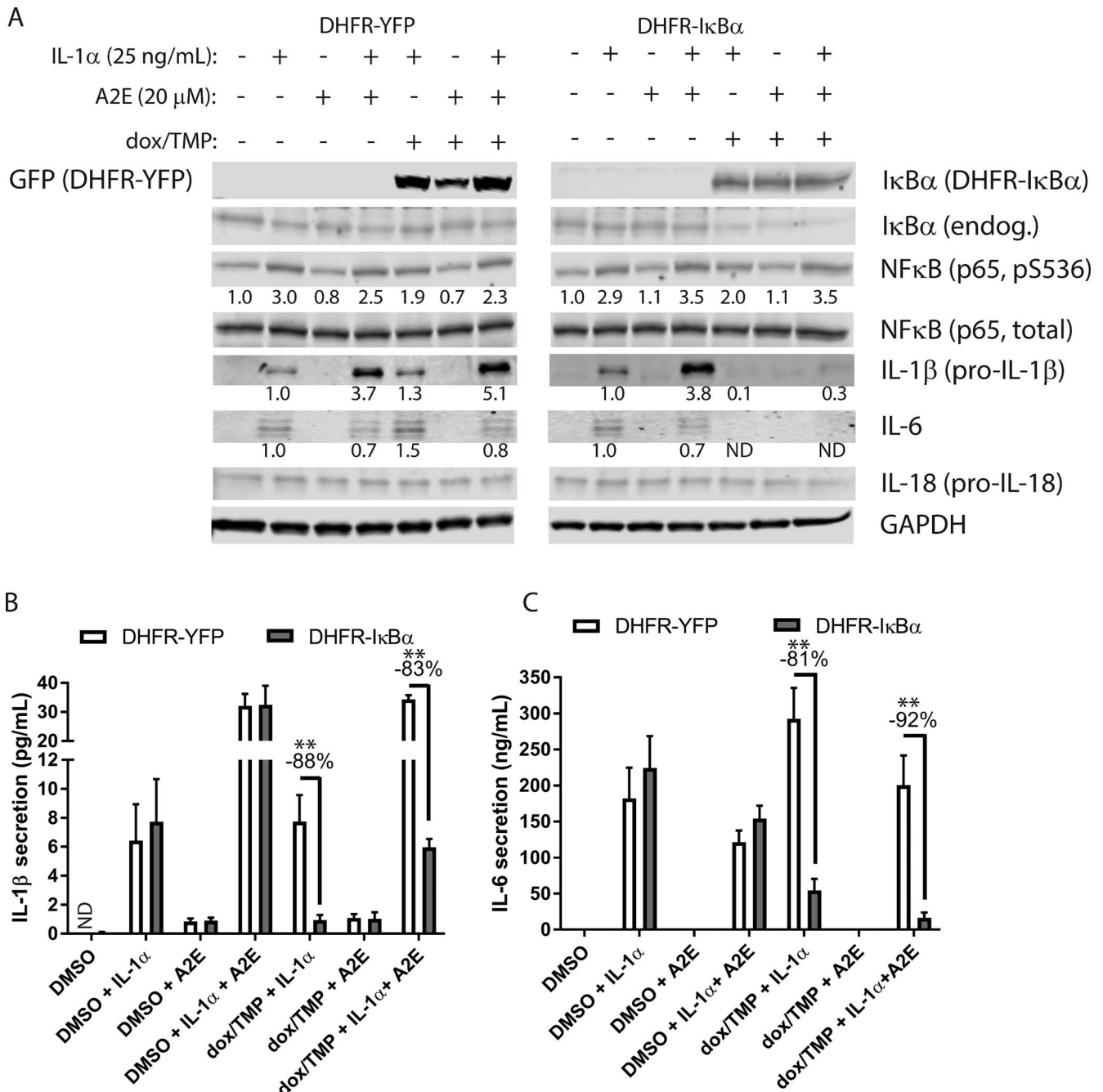


FIGURE 5. DHFR-IκBα stabilization prevents cytokine production and secretion in response to IL-1α, A2E, and the combination thereof. ARPE-19 cells were plated and allowed to achieve confluence over the course of 1 week followed by pretreatment with DMSO or dox/TMP (100 ng/mL/1 μM) for 48 hours in serum-free media, after which IL-1α (25 ng/mL) and/or A2E (20 μM) were added for an additional 24 hours. (A) Western blot of cell lysates post treatment. (B, C) ELISA probing for IL-1β (B) or IL-6 (C) in the conditioned media post treatment. *n* = 3, ***P* < 0.01, unpaired, two-tailed *t*-test assuming equal variance. Representative data shown of *n* ≥ 3 independent experiments for (A), mean ± SD for all bar graphs in this figure.

DMSO-treated DHFR-YFP and DHFR-IκBα cells from “not detected” (values at or below the blank) to 6.4 ± 2.5 and 7.7 ± 2.9 pg/mL, respectively (Fig. 5B). In contrast, A2E minimally, but consistently, increased IL-1β secretion from “not detected” to 0.8 ± 0.2 and 0.9 ± 0.2 pg/mL in DMSO-treated DHFR-YFP and DHFR-IκBα cells, respectively (Fig. 5B). As expected, the combination of NFκB priming (achieved by IL-1α treatment) and inflammasome assembly (achieved by A2E treatment) substantially increased IL-1α-mediated IL-1β secretion in DMSO-treated DHFR-YFP and DHFR-IκBα cells to 32.1 ± 4.1 and 32.5 ± 6.6 pg/mL, respectively (Fig. 5B). After

addition of dox/TMP, there were no significant changes in IL-1β secretion levels in DHFR-YFP cells treated with IL-1α, A2E, or the combination of both when compared with DMSO-treated cells (Fig. 5B). In contrast, stabilization of DHFR-IκBα significantly reduced IL-1β secretion in IL-1α-treated cells by 88% (7.7 ± 1.8 vs. 0.9 ± 0.3 pg/mL, *P* < 0.01) and similarly decreased IL-1β levels by 83% (34.3 ± 1.4 vs. 5.96 ± 0.6 pg/mL, *P* < 0.01) in IL-1α/A2E-treated cells (Fig. 5B) when compared with the corresponding DHFR-YFP control cells. A2E-mediated slight increases in IL-1β were not affected by DHFR-IκBα stabilization (Fig. 5B).

Secretion levels of IL-6 after IL-1 α treatment were substantially increased compared with DMSO-only treated cells to 182 ± 42.7 ng/mL (4666-fold) in DHFR-YFP cells and 224 ± 43.9 ng/mL (6500-fold) in DHFR-I κ B α cells (Fig. 5C). For simplicity, a zoomed-in view of low, but detectable, basal levels of IL-6 are shown in Supplemental Figure S2A. Surprisingly, treatment with A2E resulted in a consistent decrease in IL-6 secretion, irrespective of co-treatment with IL-1 α or dox/TMP (Fig. 5C, Supplemental Fig. S2A), in agreement with Western blotting (Fig. 5A), but at odds with previous observations.²² It is also important to note that treatment with dox/TMP appeared to consistently increase secreted IL-6 levels in DHFR-YFP-expressing cells (Fig. 5C), in agreement with previous studies.⁵² Stabilization of DHFR-I κ B α significantly prevented the secretion of IL-6 after IL-1 α stimulation (292.5 ± 42.7 vs. 54.4 ± 16.2 ng/mL, -81%, $P < 0.01$, Fig. 5C), A2E treatment (69.3 ± 25.5 pg/mL vs. 5.5 ± 9.5 pg/mL, -93%, $P < 0.05$, Supplemental Fig. S2A), or the combination thereof (200.5 ± 41.2 vs. 16.4 ± 7.2 ng/mL, -92%, $P < 0.01$, Fig. 5C) when compared with the corresponding DHFR-YFP control cells.

The I κ B α Destabilized Domain Strategy Can Be Used to Dampen NFκB Signaling From Multiple Initiating Stimuli

In addition to IL-1 α , a number of other pathogen-associated molecular patterns or other stimuli can trigger activation of NFκB signaling, albeit through different cell surface receptors and mechanisms. These molecules include bacterial-derived LPS, TNF α , and A2E,²² among others. We tested the ability of these stimuli to activate NFκB signaling using an ARPE-19 GLuc reporter cell line. We did not observe NFκB activation when using 4-hydroxynonenal (4-HNE), in agreement with previous observations⁵¹ (Supplemental Fig. S2B). In contrast to previous findings,²² we did not detect NFκB activation using A2E (Supplemental Fig. S2B). However, both LPS (0.1–10 μ g/mL, Fig. 6A, $P < 0.05$, $P < 0.01$) and TNF α (0.25–25 ng/mL, Fig. 6B, $P < 0.05$, $P < 0.01$) caused significant increases in the secretion of GLuc, indicating activation of NFκB. Next, we assessed whether our DHFR-I κ B α strategy was broadly applicable for dampening NFκB signaling triggered by these stimuli. ARPE-19 cells treated with LPS (10 μ g/mL, 24 hours) demonstrated an approximately 9- to 12-fold increase in *IL-1 β* transcript levels, which were significantly reduced by 75% in dox/TMP-treated DHFR-I κ B α cells (Fig. 6C, $P < 0.01$). *IL-6* transcript levels were minimally increased after LPS administration by approximately 2.5-fold in both DHFR-YFP and DHFR-I κ B α cells (DMSO-treated cells, Supplemental Fig. S2C). *IL-6* levels were further increased by 93% in DHFR-YFP cells treated with LPS/dox/TMP. However, stabilization of DHFR-I κ B α reduced *IL-6* transcript levels by 43% compared with DMSO/LPS-treated cells (Supplemental Fig. S2C). Cells treated with TNF α (2.5 ng/mL, 24 hours) showed a robust 26- to 35-fold increase in *IL-1 β* transcript levels (Fig. 6D), without any discernible effect on *IL-6* transcript levels (Supplemental Fig. S2D). Stabilization of DHFR-I κ B α significantly reduced TNF α -associated *IL-1 β* induction by 72% (Fig. 6D, $P < 0.05$). Our data highlight the general applicability of this DHFR-I κ B α system for conditionally dampening NFκB signaling in response to a variety of instigating stimuli.

DISCUSSION

We have presented a novel, small molecule-regulated strategy to conditionally prevent NFκB-mediated proinflammatory signaling using a DHFR-based destabilized domain fused to

I κ B α . To the best of our knowledge, this is the first demonstration of destabilized domain technology in RPE cells, and the first destabilized domain approach to specifically target NFκB signaling. Upon expression and stabilization of the DHFR-I κ B α fusion protein with dox/TMP, cells are protected from the proinflammatory effects of IL-1 α , TNF α , and LPS, reducing NFκB-dependent gene expression and cytokine production by approximately 80% to 90%. Suppression of NFκB signaling to this extent has been achieved previously using various small-molecule NFκB inhibitors (there are more than 700 of them identified so far²⁴) or by using a constitutively expressed “super repressor” version of I κ B α that cannot be phosphorylated or degraded after exposure to stimulus.⁵⁵ However, our approach is unique in that although it is genetically encoded, it is conditional and can be cycled “on” or “off” repeatedly at will, simply by addition or omission of an orally available small molecule or molecules. We speculate that such a regulatable strategy (which could be targeted to particular retinal cells using cell-specific promoters) will be beneficial for manipulating cellular pathways within the retina (such as stress-responses) that are otherwise difficult to accurately regulate, or have the potential for significant off-target/damaging effects if constitutively activated or repressed. We feel compelled to mention, however, that patients given TMP and sulfamethoxazole may have an increased risk of developing a drug-induced thrombocytopenia or megaloblastic anemia, especially in the immunocompromised.⁵⁴ Recently, a few cases of TMP/sulfamethoxazole-associated aseptic meningitis, as seen in some patients taking nonsteroidal anti-inflammatory drugs, have been reported, and is potentially linked to increased IL-6 release in certain contexts.⁵⁵ To evaluate the safety of a long-term regimen of TMP, future in vivo studies are warranted. Nonetheless, we are cautiously optimistic that this DHFR-based approach can safely and effectively be used in vivo^{54,55} in the eye to regulate protein abundance.

Given that NFκB regulates more than 500 genes involved in inflammation, cell growth, apoptosis, and carcinogenesis, it is difficult to predict the effects of long-term NFκB inhibition in the eye or within the RPE. Mice lacking NFκB subunit RelA/p65 (the subunit we focused on in this article) die in utero,⁵⁶ whereas NFκB/p105 null mice appear to have normally developed eyes and RPE cells, and are resistant to *Alu* RNA-mediated degeneration.⁵⁷ To complicate the situation further, a previous study found that inhibition of NFκB signaling may not affect RPE cells in a similar fashion to other commonly used cells.⁵⁸

Although we validated our DHFR-I κ B α approach by focusing primarily on IL-1 β and IL-6, both of which have been implicated in AMD,^{59–61} we also identified reductions in a number of separate genes that have previously been linked to retinal degeneration. For example, *VCAM1*, *TLR2*, and *IL-8* transcripts were all found to be substantially reduced in IL-1 α -treated cells with stabilized DHFR-I κ B α . *VCAM1* has been shown to play an important role in oxidative-stress-mediated angiogenesis in the retina⁶² and has been shown to contribute to TNF α -mediated angiogenesis.⁶³ *TLR2* has been demonstrated to potentiate inflammation originating from AMD-related carboxyethylpyrrole-adducted proteins⁶⁴ and activation of *TLR2* causes experimental choroidal neovascularization (CNV).⁶⁵ *IL-8* polymorphisms have been associated with wet AMD.^{66,67} However, inhibition of NFκB also reduced transcript levels of chemokine (C-C motif) ligand 2 (*CCL2*, also known as *MCP-1*). Mice deficient in *Ccl2* develop drusen-like deposits consisting of autofluorescent subretinal macrophages, but were less susceptible to laser-induced CNV.⁶⁸ Ultimately, to further clarify the potential benefits or detriments of long-term NFκB inhibition in the retina and its eventual relevance to

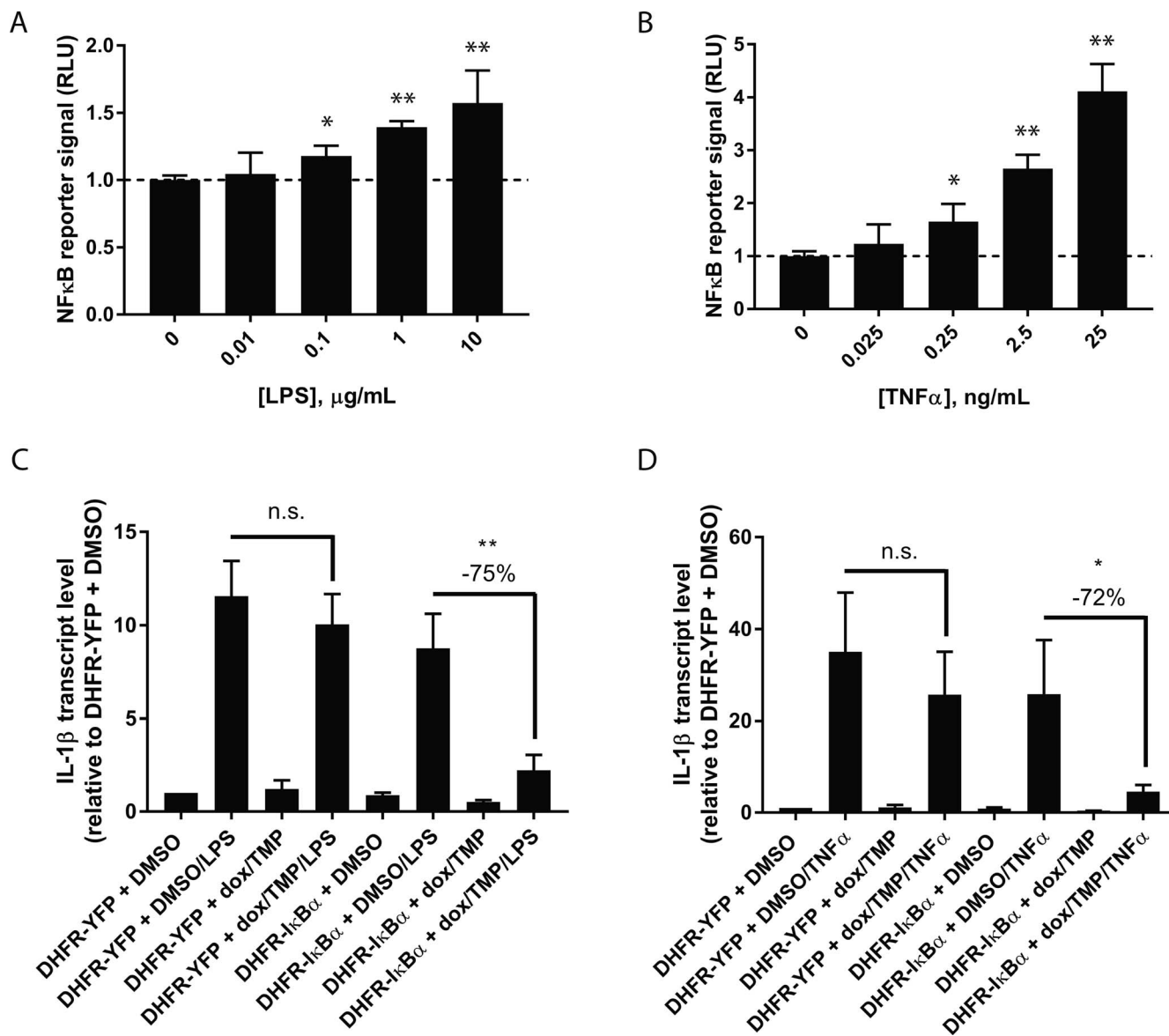


FIGURE 6. Stabilized DHFR-I κ B α also prevents LPS and TNF α -mediated NF κ B priming. (A, B) LPS and TNF α induce NF κ B activity in a dose-dependent manner. 5NF-Gluc ARPE-19 cells were treated with the indicated concentrations of LPS or TNF α for 24 hours followed by assessment of Gluc activity in the media. $n = 3$, * $P < 0.05$, ** $P < 0.01$, unpaired, one-tailed t -test assuming equal variance. (C, D). qPCR of IL-1 β transcripts \pm LPS (10 μ g/mL, 24 hours) or TNF α (2.5 ng/mL, 24 hours) \pm dox/TMP. $n = 3$, * $P < 0.05$, ** $P < 0.01$, unpaired, two-tailed t -test assuming equal variance. Mean \pm SD for all bar graphs in this figure.

retinal degeneration, we must test the DHFR-I κ B α strategy directly in mice.

NF κ B-dependent genes, such as *IL-8* and *TNF α* are clearly linked to the development of CNV; however, we also believe that DHFR-I κ B α -mediated NF κ B inhibition could protect against inflammasome-mediated “dry” AMD-related symptoms, such as geographic atrophy.⁵⁷ Because NF κ B-dependent “priming” not only produces inflammatory pro-cytokines, but also transcriptionally upregulates NLRP3,⁶⁹ a necessary component required for the NLRP3 inflammasome complex, DHFR-I κ B α -mediated inhibition of NF κ B priming, in theory, could also indirectly modulate inflammasome assembly. NLRP3 is unique when compared with other NLRPs, such as NLRP1 or NLRP6, in that its basal level of expression is generally not sufficient for inflammasome activation in resting cells.⁶⁹ Surprisingly, NLRP3 expression in ARPE-19 cells is postulated to be constitutive,¹⁹ not necessarily inducible, and thus

possibly NF κ B-independent in these immortalized cells. Nonetheless, we indeed found that our DHFR-I κ B α method significantly prevented IL-1 α -primed, A2E-exacerbated secretion of IL-1 β . It is yet to be determined whether this inhibition is due solely to prevention of inflammasome priming, inflammasome assembly, or both, which is a topic for future studies.

In summary, our current study demonstrates a proof-of-principle use of DHFR-I κ B α to prevent NF κ B-mediated inflammatory signaling in cultured RPE cells. Ultimately, we envision that a DHFR or alternative destabilized domain-based strategy could effectively be used to temporally and conditionally control a number of different signaling pathways (including inflammation) in different tissues in the eye, and is therefore an exciting tool for potentially treating retinal diseases caused by diverse genetic or environmental insults.

Acknowledgments

Supported in part by an endowment from the Roger and Dorothy Hirl Research Fund (JDH), a vision research grant from the Karl Kirchgessner Foundation (JDH), a National Eye Institute Visual Science Core Grant (EY020799), an unrestricted grant from Research to Prevent Blindness, a Career Development Award from Research to Prevent Blindness (JDH), and a Research to Prevent Blindness Medical Student Eye Research Fellowship (KTV).

Disclosure: **K.T. Vu**, None; **F. Zhang**, None; **J.D. Hulleman**, None

References

- Vallabhapurapu S, Karin M. Regulation and function of NF- κ B transcription factors in the immune system. *Annu Rev Immunol.* 2009;27:693-733.
- Lan W, Petznick A, Heryati S, Rifada M, Tong L. Nuclear Factor- κ B: central regulator in ocular surface inflammation and diseases. *Ocul Surf.* 2012;10:137-148.
- Chen M, Xu H. Parainflammation chronic inflammation, and age-related macular degeneration. *J Leukoc Biol.* 2015;98:713-725.
- Moon MR, Parikh AA, Pritts TA, et al. Complement component C3 production in IL-1 β -stimulated human intestinal epithelial cells is blocked by NF- κ B inhibitors and by transfection with ser 32/36 mutant I κ B α . *J Surg Res.* 1999;82:48-55.
- Cogswell JP, Godlevski MM, Wisely GB, et al. NF- κ B regulates IL-1 β transcription through a consensus NF- κ B binding site and a nonconsensus CRE-like site. *J Immunol.* 1994;153:712-723.
- Libermann TA, Baltimore D. Activation of interleukin-6 gene expression through the NF- κ B transcription factor. *Mol Cell Biol.* 1990;10:2327-2334.
- Patel MN, Carroll RG, Galvan-Pena S, et al. Inflammasome priming in sterile inflammatory disease. *Trends Mol Med.* 2017;23:165-180.
- Napetschnig J, Wu H. Molecular basis of NF- κ B signaling. *Annu Rev Biophys.* 2013;42:443-468.
- Renner F, Schmitz ML. Autoregulatory feedback loops terminating the NF- κ B response. *Trends Biochem Sci.* 2009;34:128-135.
- Fagerlund R, Behar M, Fortmann KT, Lin YE, Vargas JD, Hoffmann A. Anatomy of a negative feedback loop: the case of I κ B α . *J R Soc Interface.* 2015;12:0262.
- Hayden MS, West AP, Ghosh S. NF- κ B and the immune response. *Oncogene.* 2006;25:6758-6780.
- de Winther MP, Kanters E, Kraal G, Hofker MH. Nuclear factor κ B signaling in atherosclerosis. *Arterioscler Thromb Vasc Biol.* 2005;25:904-914.
- Schreiber S, Nikolaus S, Hampe J. Activation of nuclear factor κ B inflammatory bowel disease. *Gut.* 1998;42:477-484.
- Simmonds RE, Foxwell BM. Signalling, inflammation and arthritis: NF- κ B and its relevance to arthritis and inflammation. *Rheumatology (Oxford).* 2008;47:584-590.
- Karin M. NF- κ B as a critical link between inflammation and cancer. *Cold Spring Harb Perspect Biol.* 2009;1:a000141.
- Halle A, Hornung V, Petzold GC, et al. The NALP3 inflammasome is involved in the innate immune response to amyloid- β . *Nat Immunol.* 2008;9:857-865.
- Martinon F, Petrilli V, Mayor A, Tardivel A, Tschopp J. Gout-associated uric acid crystals activate the NALP3 inflammasome. *Nature.* 2006;440:237-241.
- Tarallo V, Hirano Y, Gelfand BD, et al. DICER1 loss and Alu RNA induce age-related macular degeneration via the NLRP3 inflammasome and MyD88. *Cell.* 2012;149:847-859.
- Tseng WA, Thein T, Kinnunen K, et al. NLRP3 inflammasome activation in retinal pigment epithelial cells by lysosomal destabilization: implications for age-related macular degeneration. *Invest Ophthalmol Vis Sci.* 2013;54:110-120.
- Rhoads JP, Lukens JR, Wilhelm AJ, et al. Oxidized low-density lipoprotein immune complex priming of the Nlrp3 inflammasome involves TLR and Fc γ R cooperation and is dependent on CARD9. *J Immunol.* 2017;198:2105-2114.
- Franchi L, Eigenbrod T, Munoz-Planillo R, et al. Cytosolic double-stranded RNA activates the NLRP3 inflammasome via MAVS-induced membrane permeabilization and K⁺ efflux. *J Immunol.* 2014;193:4214-4222.
- Anderson OA, Finkelstein A, Shima DT. A2E induces IL-1 β production in retinal pigment epithelial cells via the NLRP3 inflammasome. *PLoS One.* 2013;8:e67263.
- Radu RA, Hu J, Yuan Q, et al. Complement system dysregulation and inflammation in the retinal pigment epithelium of a mouse model for Stargardt macular degeneration. *J Biol Chem.* 2011;286:18593-18601.
- Gupta SC, Sundaram C, Reuter S, Aggarwal BB. Inhibiting NF- κ B activation by small molecules as a therapeutic strategy. *Biochim Biophys Acta.* 2010;1799:775-787.
- Song C, Mitter SK, Qi X, et al. Oxidative stress-mediated NF- κ B phosphorylation upregulates p62/SQSTM1 and promotes retinal pigmented epithelial cell survival through increased autophagy. *PLoS One.* 2017;12:e0171940.
- Wang L, Cano M, Handa JT. p62 provides dual cytoprotection against oxidative stress in the retinal pigment epithelium. *Biochim Biophys Acta.* 2014;1843:1248-1258.
- Cooley CB, Ryno LM, Plate L, et al. Unfolded protein response activation reduces secretion and extracellular aggregation of amyloidogenic immunoglobulin light chain. *Proc Natl Acad Sci U S A.* 2014;111:13046-13051.
- Ryno LM, Genereux JC, Naito T, et al. Characterizing the altered cellular proteome induced by the stress-independent activation of heat shock factor 1. *ACS Chem Biol.* 2014;9:1273-1283.
- Chen JJ, Genereux JC, Qu S, Hulleman JD, Shoulders MD, Wiseman RL. ATF6 activation reduces the secretion and extracellular aggregation of destabilized variants of an amyloidogenic protein. *Chem Biol.* 2014;21:1564-1574.
- Shoulders MD, Ryno LM, Cooley CB, Kelly JW, Wiseman RL. Broadly applicable methodology for the rapid and dosable small molecule-mediated regulation of transcription factors in human cells. *J Am Chem Soc.* 2013;135:8129-8132.
- Shoulders MD, Ryno LM, Genereux JC, et al. Stress-independent activation of XBP1s and/or ATF6 reveals three functionally diverse ER proteostasis environments. *Cell Rep.* 2013;3:1279-1292.
- Iwamoto M, Björklund T, Lundberg C, Kirik D, Wandless TJ. A general chemical method to regulate protein stability in the mammalian central nervous system. *Chem Biol.* 2010;17:981-989.
- Hulleman JD, Brown SJ, Rosen H, Kelly JW. A high-throughput cell-based Gaussia luciferase reporter assay for identifying modulators of fibulin-3 secretion. *J Biomol Screen.* 2013;18:647-658.
- Badr CE, Niers JM, Tjon-Kon-Fat LA, Noske DP, Wurdinger T, Tannous BA. Real-time monitoring of nuclear factor κ B activity in cultured cells and in animal models. *Mol Imaging.* 2009;8:278-290.
- Luo Y, Hara T, Ishido Y, et al. Rapid preparation of high-purity nuclear proteins from a small number of cultured cells for use in electrophoretic mobility shift assays. *BMC Immunol.* 2014;15:586.
- Nguyen A, Hulleman JD. Differential tolerance of 'pseudo-pathogenic' tryptophan residues in calcium-binding EGF

- domains of short fibulin proteins. *Exp Eye Res.* 2015;130:66-72.
37. Hulleman JD, Balch WE, Kelly JW. Translational attenuation differentially alters the fate of disease-associated fibulin proteins. *FASEB J.* 2012;26:4548-4560.
 38. Hulleman JD, Kaushal S, Balch WE, Kelly JW. Compromised mutant EFEMP1 secretion associated with macular dystrophy remedied by proteostasis network alteration. *Mol Biol Cell.* 2011;22:4765-4775.
 39. Chiao PJ, Miyamoto S, Verma IM. Autoregulation of I kappa B alpha activity. *Proc Natl Acad Sci U S A.* 1994;91:28-32.
 40. Osborn L, Kunkel S, Nabel GJ. Tumor necrosis factor alpha and interleukin 1 stimulate the human immunodeficiency virus enhancer by activation of the nuclear factor kappa B. *Proc Natl Acad Sci U S A.* 1989;86:2336-2340.
 41. Di Paolo NC, Shayakhmetov DM. Interleukin 1alpha and the inflammatory process. *Nat Immunol.* 2016;17:906-913.
 42. Ghosh S, May MJ, Kopp EB. NF-kappa B and Rel proteins: evolutionarily conserved mediators of immune responses. *Ann Rev Immunol.* 1998;16:225-260.
 43. Hiscott J, Marois J, Garoufalos J, et al. Characterization of a functional NF-kappa B site in the human interleukin 1 beta promoter: evidence for a positive autoregulatory loop. *Mol Cell Biol.* 1993;13:6231-6240.
 44. Puren AJ, Fantuzzi G, Dinarello CA. Gene expression, synthesis, and secretion of interleukin 18 and interleukin 1beta are differentially regulated in human blood mononuclear cells and mouse spleen cells. *Proc Natl Acad Sci U S A.* 1999;96:2256-2261.
 45. Wu JM, Xu Y, Skill NJ, et al. Autotaxin expression and its connection with the TNF-alpha-NF-kappaB axis in human hepatocellular carcinoma. *Mol Cancer.* 2010;9:71.
 46. Catz SD, Johnson JL. Transcriptional regulation of bcl-2 by nuclear factor kappa B and its significance in prostate cancer. *Oncogene.* 2001;20:7342-7351.
 47. Sparrow JR, Parish CA, Hashimoto M, Nakanishi K. A2E, a lipofuscin fluorophore, in human retinal pigmented epithelial cells in culture. *Invest Ophthalmol Vis Sci.* 1999;40:2988-2995.
 48. Schutt F, Bergmann M, Kopitz J, Holz FG. Detergent-like effects of the lipofuscin retinoid component A2-E in retinal pigment epithelial cells [in German]. *Ophthalmologe.* 2002;99:861-865.
 49. Sakurai H, Chiba H, Miyoshi H, Sugita T, Toriumi W. IkappaB kinases phosphorylate NF-kappaB p65 subunit on serine 536 in the transactivation domain. *J Biol Chem.* 1999;274:30353-30356.
 50. Sasaki CY, Barberi TJ, Ghosh P, Longo DL. Phosphorylation of RelA/p65 on serine 536 defines an I{kappa}B{alpha}-independent NF-{kappa}B pathway. *J Biol Chem.* 2005;280:34538-34547.
 51. Pradere JP, Hernandez C, Koppe C, Friedman RA, Luedde T, Schwabe RF. Negative regulation of NF-kappaB p65 activity by serine 536 phosphorylation. *Sci Signal.* 2016;9:ra85.
 52. Antonen J, Saha H, Hulkkonen J, Lumio J, Pasternack A, Hurme M. Increased in vitro production of interleukin 6 in response to trimethoprim among persons with trimethoprim induced systemic adverse reactions. *J Rheumatol.* 1999;26:2585-2590.
 53. Jobin C, Panja A, Hellerbrand C, et al. Inhibition of proinflammatory molecule production by adenovirus-mediated expression of a nuclear factor kappaB super-repressor in human intestinal epithelial cells. *J Immunol.* 1998;160:410-418.
 54. Hesdorffer CS, Longo DL. Drug-induced megaloblastic anemia. *N Engl J Med.* 2015;373:1649-1658.
 55. Jha P, Stromich J, Cohen M, Wainaina JN. A rare complication of trimethoprim-sulfamethoxazole: drug induced aseptic meningitis. *Case Rep Infect Dis.* 2016;2016:3879406.
 56. Beg AA, Baltimore D. An essential role for NF-kappaB in preventing TNF-alpha-induced cell death. *Science.* 1996;274:782-784.
 57. Kerur N, Hirano Y, Tarallo V, et al. TLR-independent and P2X7-dependent signaling mediate Alu RNA-induced NLRP3 inflammasome activation in geographic atrophy. *Invest Ophthalmol Vis Sci.* 2013;54:7395-7401.
 58. Yang P, McKay BS, Allen JB, Jaffe GJ. Effect of NF-kappa B inhibition on TNF-alpha-induced apoptosis in human RPE cells. *Invest Ophthalmol Vis Sci.* 2004;45:2438-2446.
 59. Seddon JM, George S, Rosner B, Rifai N. Progression of age-related macular degeneration: prospective assessment of C-reactive protein, interleukin 6, and other cardiovascular biomarkers. *Arch Ophthalmol.* 2005;123:774-782.
 60. Izumi-Nagai K, Nagai N, Ozawa Y, et al. Interleukin-6 receptor-mediated activation of signal transducer and activator of transcription-3 (STAT3) promotes choroidal neovascularization. *Am J Pathol.* 2007;170:2149-2158.
 61. Zhao M, Bai Y, Xie W, et al. Interleukin-1beta level is increased in vitreous of patients with neovascular age-related macular degeneration (nAMD) and polypoidal choroidal vasculopathy (PCV). *PLoS One.* 2015;10:e0125150.
 62. Dong A, Shen J, Zeng M, Campochiaro PA. Vascular cell-adhesion molecule-1 plays a central role in the proangiogenic effects of oxidative stress. *Proc Natl Acad Sci U S A.* 2011;108:14614-14619.
 63. Kim TK, Park CS, Na HJ, et al. Ig-like domain 6 of VCAM-1 is a potential therapeutic target in TNF-alpha-induced angiogenesis. *Exp Mol Med.* 2017;49:e294.
 64. Saeed AM, Duffort S, Ivanov D, et al. The oxidative stress product carboxyethylpyrrole potentiates TLR2/TLR1 inflammatory signaling in macrophages. *PLoS One.* 2014;9:e106421.
 65. West XZ, Malinin NL, Merkulova AA, et al. Oxidative stress induces angiogenesis by activating TLR2 with novel endogenous ligands. *Nature.* 2010;467:972-976.
 66. Ricci F, Staurengi G, Lepre T, et al. Haplotypes in IL-8 gene are associated to age-related macular degeneration: a case-control study. *PLoS One.* 2013;8:e66978.
 67. Tsai YY, Lin JM, Wan L, et al. Interleukin gene polymorphisms in age-related macular degeneration. *Invest Ophthalmol Vis Sci.* 2008;49:693-698.
 68. Luhmann UF, Robbie S, Munro PM, et al. The drusenlike phenotype in aging Ccl2-knockout mice is caused by an accelerated accumulation of swollen autofluorescent subretinal macrophages. *Invest Ophthalmol Vis Sci.* 2009;50:5934-5943.
 69. Bauernfeind FG, Horvath G, Stutz A, et al. Cutting edge: NF-kappaB activating pattern recognition and cytokine receptors license NLRP3 inflammasome activation by regulating NLRP3 expression. *J Immunol.* 2009;183:787-791.